


Study of Resonance Helical Magnetic Field (RHF) Effect In IR-T1 Tokamak Plasma Using Hilbert-Huang Transform

H. Faridyousefi¹ M.K. Salem^{1*} M.Ghoranneviss¹ ¹ Plasma Physics Research Center, Science and Research Branch, Islamic Azad University, Tehran, 1477893855, Iran

ABSTRACT

In the IR-T1 Tokamak the effect of a resonance helical magnetic field (RHF) on plasma confinement are presented using Hilbert-Huang Transform method. Mirnov coil data analyzed by Hilbert-Huang Transform (HHT) and decomposed to the main intrinsic mode functions (imfs) and their instantaneous frequencies (IFs). We find that, HHT method can extract MHD activities with different amplitudes in the different times. Then, the IFs of these modes can be calculated by Hilbert Transform (HT). As a comparison of WT and HHT analysis the Hilbert spectrum has much better frequency definition. Amplitude modulation of Mironov oscillations in IR-T1 tokamak plasma generate intra-wave frequency modulation, In the Hilbert spectrum analysis this effect is small compared to the STFT and WT spectrums. In our study, Magnetic islands with frequency around 40 kHz can be seen in wavlet Transform (WT) and HHT results in ohmic and RHF discharges. The HHT results after application of $l=2/n=1$ resonant field show that, the amplitude of $m=2$ poloidal MHD mode are amplified and then suppressed for a few milliseconds after amplification. Similarly, the amplitude of the $m=3$ MHD mode are amplified and then strongly suppressed by the start of the $l=3/n=1$ resonant field.

Keyword: Structured Stainless Steel, Reduce Stress Shielding

©2021 The Authors. Published by Fundamental Journals. This is an open-access article under the CC BY-NC
<https://creativecommons.org/licenses/by-nc/4.0/>

INTRODUCTION

The effect of resonant helical magnetic field (on plasma stability and confinement) is of great interest in the field of plasma physics research [1-5]. Using external coils around the tokamak plasma chamber creates resonant magnetic field perturbations (RHF). This external field may strongly affect the plasma dynamics by stabilizing the MHD activity accompanied with disruptions at higher applied fields [1] and locking of modes leading

eventually to disruption of the plasma [3]. The RHF induced stabilization of rotating $m = 2/n = 1$ MHD mode observed in COMPASS-C in low density with low-q plasmas [1]. In this tokamak natural (2,1) mode decayed into the noise as soon as the RHF field is applied. The experimental results show that, after application of resonant helical field (RHF) rotating frequency of the magnetic islands is reduced because of mode stabilization [4]. It has been found that the

reduction of mode frequency correlates with a reduction in mode amplitude rather than with the RHF amplitude [4].

Tearing mode instability is responsible for various types of disruptions in the tokamak plasma [4]. The growth of (2,1) tearing mode could be influenced by applying a perturbative magnetic field produced by an ($l = 2, n = 1$) resonant helical coil [3].

In tearing mode instability, with the sufficiently high local resistivity, energy can be dissipated during the reconnection process changing the magnetic field topology. This occurs at surfaces with rational value of $q = m/n$ (m and n are the poloidal and toroidal mode number). At these surfaces the magnetic field lines break and reconnect to form magnetic islands. In many tokamaks, the major disruptions are caused by the interaction of $m = 2/n = 1$ magnetic islands with the limiter or with the cold plasma at the edge [2]. Also, density limit disruptions have been reported that are associated with coupling of a growing (2,1) island with (1,1) mode [6].

Other theory suggests that the major disruptions are triggered by the coupling of a growing (2,1) island with (1,1) mode or with (3,2) mode [6, 7].

In addition, the external helical field suppressed the MHD activities in the STORM-M tokamak discharges. In this tokamak during low- q ohmic discharges with the high MHD activity, amplitude and frequency of (2,1) mirnov fluctuations are significantly reduced after the activation of resonant field. A significant reduction in mirnov oscillation is observed as the magnitude of the RHF is increased [4]. In J-TEXT tokamak experiments with increasing RMP amplitude, the mode stabilization is first observed but a large mode locking is occurred if the RMP amplitude is increased to a very large value [8].

Mode-locking is occurred when magnetic probe signal grows initially in response to the instability. It reaches a maximum and begins to fall when the coupling to the wall starts to reduce the frequency. In other words, if the wave amplitude is sufficiently large so the plasma interacts with external conductors, such as the vacuum vessel, it results in an increasingly rapid transfer of momentum from the plasma and then, the mode propagation slows down to a halt [9, 10].

In addition, in J-TEXT tokamak, several experimental results were obtained including partial or complete suppression of the existing $m = 2/n = 1$ tearing mode and non-uniform MHD oscillations [11]. In the tokamak experiments, MHD mode stabilization, mode suppression and mode locking are accompanied by reduction of the mode amplitude and mode frequency. Therefore, in our study the effects of static resonance helical field produced by ($l = 2, n = 1$) and ($l = 3, n = 1$) helical coils on the (2,1) and (3,1) island is

investigated experimentally and analyzed by using Hilbert-Huang Transform. This method decomposes tokamak data such as mirnov signals to the main functions and their instantaneous frequencies. Tokamak experimental data exhibit nonstationary and nonlinear characteristics in MHD instabilities and turbulence fluctuations. In this process, the frequency of the oscillations is not constant and may vary with time. The investigation of such time-dependent oscillations requires advanced time-frequency analysis approaches such as short time Fourier transform [12] wavelet transform [13] and Hilbert-Huang Transform [14]. Huang and coworkers introduced empirical mode decomposition (EMD) method for data analysis in 1998 [14]. This approach consists of two parts of data analysis of the problem. First, EMD decomposes the original data into a series of intrinsic mode functions (imfs). An imf is any function with the same number of extrema and zero crossings, with its envelopes being symmetric about zero. Second, the instantaneous frequency can be obtained by Hilbert Spectral analysis. These two separate parts, known as (HHT) method.

In the field of plasma physics the EMD method has been successfully applied. The application of empirical mode decomposition to the analysis of solar coronal oscillations was investigated [15].

EMD method combined with Hilbert-Huang power spectrum was applied to analyze nonstationary signals of a Hall-effect thruster plasma [16]. In addition, the time-frequency analysis of tokamak signals particularly edge fluctuation data and magnetic probe signals are analyzed by HHT method [17-22].

For example, Kakurin and Orlovsky proposed this method to decompose complex tearing instability to separate tearing-mode by the MHD-diagnostic data processing. They also analyzed the signals from mirnov coil in investigation the dynamic behavior of large-scale MHD perturbations in the T-10 tokamak. They applied the empirical mode decomposition method to expand a multimode MHD perturbations in individual modes [17, 18]. Jha and coworkers applied the HHT method to analyze different kinds of ADITYA tokamak data such as fluctuations in floating potential and ion-saturation current measured by Langmuir probes in scrape off layer (SOL) and edge plasma. ADITYA mirnov coil data have been decomposed into imfs and only two of the several imfs are strongly correlated with the raw data. First, a single stationary mode oscillates at 10 kHz. Second, an intermittent mode about at 30 kHz also appears [19]. Capabilities of the EMD as a tool for turbulence and MHD instability analysis explored in the ISTTOK tokamak. Coelho and his coworker reported that this technique proves to be particularly suited for the typically bursty activity in

both MHD activity and turbulence fluctuations in ISTTOK tokamak pulses. They studied HHT analysis of mirnov coil signal in the vicinity of $m = 2$ mode destabilization and indicated that, only five imfs were enough to describe the magnetic coil data analysis. In such pulses, the MHD activity as measured from the magnetic coils, indicated prevalently a mixture of $m = 3/4$ [20]. The improved Hilbert-Huang transform has been introduced in detail as a novel time-frequency tool to analyze experimental signals in the HL-2A and SUNIS tokamaks. For example, they indicated that, the coupling MHD modes are mainly in the frequency range of 10-20 kHz. Moreover, a high frequency mode with frequency about 35 kHz and low amplitude can be detected by the improved HHT clearly [21]. Therefore, despite its effectiveness, HHT analysis has not been used extensively and is necessary to use this method to analyze the raw data of other tokamaks. In addition, the short-time Fourier transform (STFT) uses a fixed window to capture the non-stationarity and thus suffers from the limited frequency resolution. On the other hand, wavelet transform (WT) can be regarded as a technique of projecting the data on to a series of a priori basic functions. Because the basic function must be predefined, the successful application of WT largely depends on the user's experience including the selection of parent wavelet and discretization of scales [23]. In Sec.2, the structure of the EMD and HT is studied. In Sec.3, The Influence of the resonance helical magnetic field on IR-T1 plasma is presented. The experimentally raw data as measured from Mironov coil is analyzed by HHT and decomposed to main intrinsic mode functions (imfs) and their instantaneous frequencies (IFs).

To evaluate the quality of the HHT method, the frequency content of Mironov oscillations is analyzed by the using Fast Fourier Transform (FFT) in ohmic and RHF discharges. For more information, time-frequency analysis of MHD activity is Investigated by STFT and CWT in these discharges and the analyses results are compared with HHT results. At the end in Sec.4, the conclusions are represented.

DESCRIPTION OF THE METHOD

The procedure of expansion of the signal $x(t)$ into intrinsic modes is known as the EMD, which was first proposed by Huang and co-workers [14]. EMD is a data-driven procedure for nonstationary and nonlinear data without a priori defined basic function[14]. In this section we briefly summarize the decomposition procedure [14, 16].

An intrinsic mode function must satisfy two conditions: (a) the number of zero crossings and extrema must either match or differ at most by one; (b) each *imf* (t) has to be symmetric with respect to its local mean value

which must tend to zero at any point. The iterative routine that permits to calculate all *imfi*(t) is called the sifting algorithm. First the local maxima, respectively, minima, of the primary signal $x(t)$ are connected by spline interpolation. This gives approximated wave forms of the upper *upp*(t) and lower *low*(t) envelopes.

Then a running mean $m_0(t) = \frac{[upp(t)+low(t)]}{2}$ and the difference $h_0(t) = x(t) - m_0(t)$ are computed.

If $h_0(t)$ does not satisfy the conditions to be an *imf*, the calculation of upper and lower envelopes is repeated, now for $h_0(t)$ treated as input data and producing $h_1(t)$. then by iteration $h_k(t) = h_{k-1}(t) - m_{k-1}(t)$. The procedure continues until $h_k(t)$ can be regarded as *imfi*(t). Now, the residue $r_1(t) = x(t) - imf_1(t)$ is calculated. The residue $r_1(t)$ is the starting point for calculation of the next intrinsic mode function *imf*₂(t). The routine is continued in the same manner for the subsequent residue $r_i(t)$ giving a set [*imfi*(t)]. The procedure stops when the last residue becomes a monotonic function of time. Finally, we can write

$$x(t) = \sum_{i=1}^n imf_i(t) + r_n(t) \quad (1)$$

Where $r_n(t)$ denotes the last residue, which cannot be farther decomposed and represents a mean trend or a shift (if constant). The EMD method does not generally provide a unique decomposition into *imf*. The outcome depends upon the stopping criterion that define the number of iteration. in other to stop the sifting procedure, to extract an *imf*, conditions (a) and (b) must be fulfil simultaneously. For any mono-component signal $x(t)$, the complex analytic form $z(t)$ of the signal can be constructed by Hilbert transform

$$z(t) = x(t) + iH[x(t)] = a(t)e^{i\phi(t)} \quad (2)$$

Where in $H[x(t)] = (P/\pi) \int_{-\infty}^{\infty} \frac{x(s)}{t-s} ds$, s is the variable of integration and P denotes the Cauchy principal value; $i = \sqrt{-1}$; and the instantaneous amplitude and phase are given by

$$a(t) = \sqrt{x(t)^2 + \{H[x(t)]\}^2}, \quad (3)$$

$$\phi(t) = \tan^{-1}\{H[x(t)]/x(t)\}, \quad (4)$$

Based on Eq. (3) and Eq (4), instantaneous frequency (IF) is defined as the derivative of the instantaneous phase

$$\nu(t) = \frac{1}{2\pi} \frac{d}{dt} \phi(t) \quad (5)$$

The above definition of $\nu(t)$ is generally accepted, however, for the discussion of its usefulness and possible interpretations the reader can refer to [14].

IR-T1 TOKAMAK MIRNOV COIL EXPERIMENTAL RESULTS AND DISCUSSION

IR-T1 tokamak is a small circular cross-sectional research tokamak located at Plasma Physics Research Center (PPRC). The tokamak has major and minor radius of 45cm and 12.5cm, respectively. The maximum achieved plasma current is 30 kA. Toroidal magnetic field induction is $B_t = 0.8 T$, the discharge time is 35 ms, and the mean electron density is $1.5 \times 10^{19} m^{-3}$. IR-T1 is equipped with poloidal array consisted of 12 coils which are separated by 30° . These discrete Mirnov coils are used to detect magnetic fluctuations and pick up the poloidal component dB/dt . The signal from each coil can be recorded by Oscilloscope (four channels) with 20 MS/s sampling rate and Data Acquisition with 2 MS/s sampling rate. Mirnov coil data of the different shots were selected and poloidal magnetic field oscillation, B_θ as measured by Mirnov coil was analyzed and the result are presented in this paper. Evidence of MHD instabilities at low value of edge safety factor $q(a)$ has been previously reported in the IR-T1 Tokamak [24, 25]. The RHF in IR-T1 tokamak is an external magnetic field which can improve the plasma confinement. This field is produced by two winding with optimized geometry conductors wound externally around the tokamak torus with a given helicity.

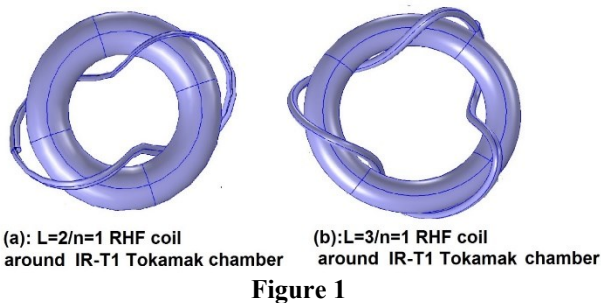


Figure 1

Figures 1a and 1b show typical schematics of the $l = 2/n = 1$ and $l = 3/n = 1$ RHF winding coil around the chamber.

The minor radius of this helical windings is 22cm ($l = 2/n = 1$) and 23 cm ($l = 3/n = 1$) and major radius is 50 cm where l and n present the numbers of toroidal and poloidal turns respectively. In the experiments presented here, the current through the helical windings was between 100-400 A.

Figure 2 shows temporal evolution of the plasma current (Fig 2a), the corresponding Mirnov signals (Fig 2b), loop voltage (Fig 2c), Hard X ray radiation (Fig 2d) and edge safety factor (Fig 2e) for shot 97425-12. In this work, the ohmic discharge during shot 9576-5 and the effect of a helical current pulse during

discharges (9576 – 6, 9576 – 7 for $l = 2/n = 1$ RHF) and (9576 – 8, 9576 – 9 for $l = 3/n = 1$ RHF) will be considered for study of the resonance helical magnetic field (RHF) effect in IR-T1 tokama plasma.

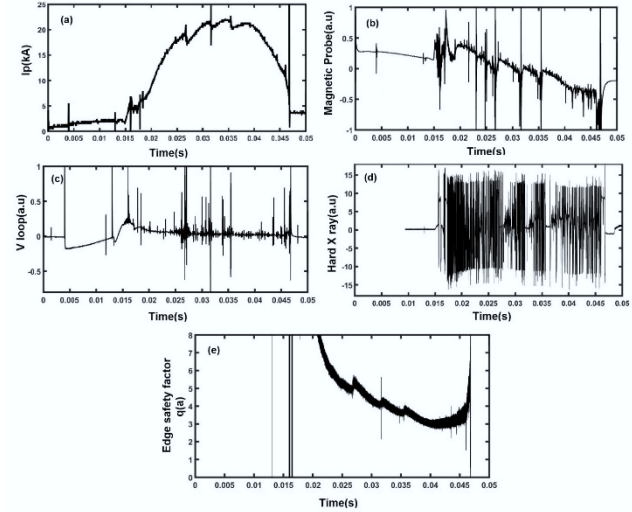


Figure 2

In addition, we used to shoot (961011 – 7 for $l = 2/n = 1$ RHF) and shot (961011-8 for $l = 3/n = 1$) to determine the spatial mode structure of MHD activity in IR-T1 tokamak plasma. The resonance helical magnetic field on IR-T1 tokamak plasma was induced by a helical current pulse of about 15ms experimentally. The resonance magnetic field was applied approximately at 25 ms for about 15 ms during the plasma current plateau.

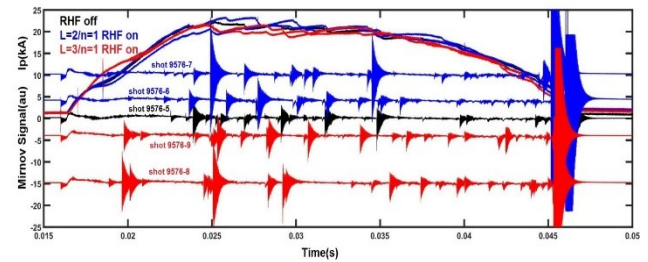


Figure 3

Figure 3 show the plasma currents and Mirnov oscillations in ohmic discharge (black line) and discharges with application of $l = 2/n = 1$ RHF (blue line), $l = 3/n = 1$ RHF (red line).

Figures 4, 5 and 6 present the results of EMD applied to the signals recorded by Mirnov coil in IR-T1 tokamak plasma. We used EMD code in references 28 for data analysis. Mirnov coil signal was decomposed into a finite number of discrete modes (see Fig 4,5,6) and the correlation coefficients between Mirnov data and different imfs in the ohmic discharge and discharges with application of RHF are obtained.

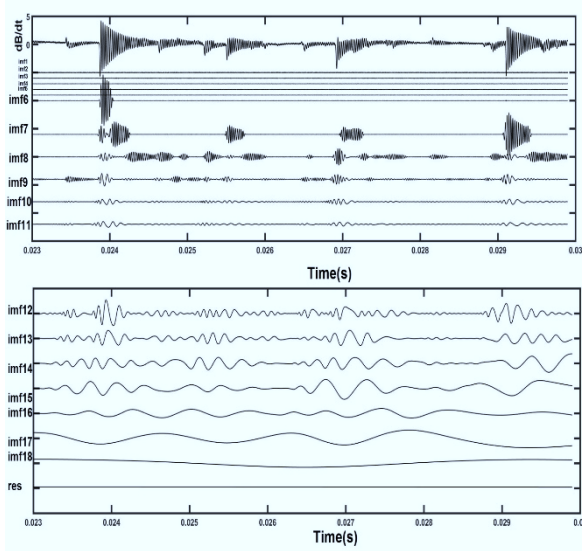


Figure 4

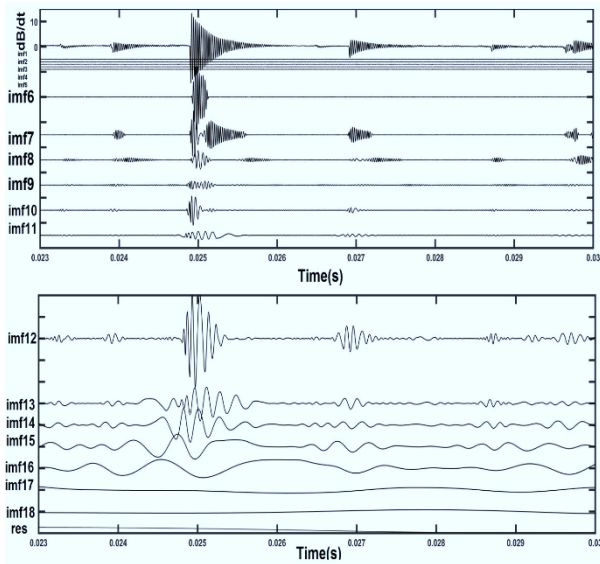


Figure 5

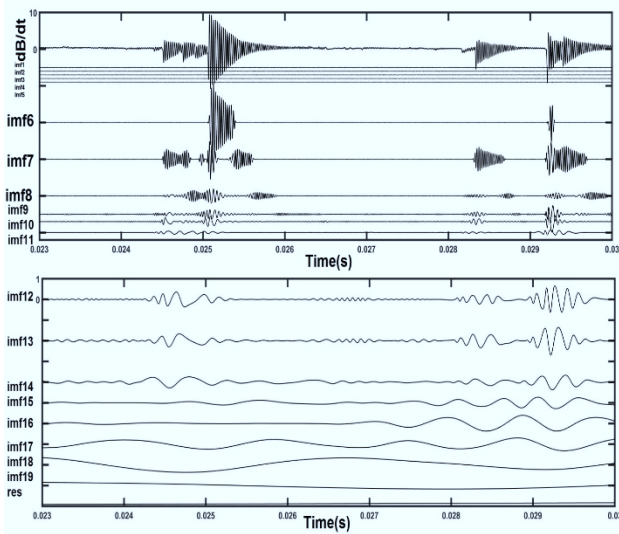


Figure6

The results show that, the amplitude of modes in the Multimode MHD activity as measured from Mirnov coil signal are different. EMD method allows to decompose data to the main intrinsic mode functions(imfs) and to determine the amplitude of the separated modes. Therefore, EMD technique can be used to determine the amplitude of each mode in the ensemble of MHD modes. A physically meaningful *imf* will have significant correlation with the mirnov coil data. We define the correlation coefficient as

$$C_{ximf_i} = \frac{\int X(t)imf_i(t)dt}{\sqrt{\int X^2(t)dt \int imf_i^2(t)dt}} \quad (6)$$

In the above definition, C_{ximf_i} has a range $[0,1]$ and we can easily identify a threshold for physically meaningful correlation coefficients.

Figure 7a shows correlation coefficients between Mirnov data and different imfs in the ohmic discharge and discharges with application of the resonance helical magnetic field. It is observed that in the ohmic discharge, imf7 is strongly correlated with the raw data with correlation coefficients 0.63.

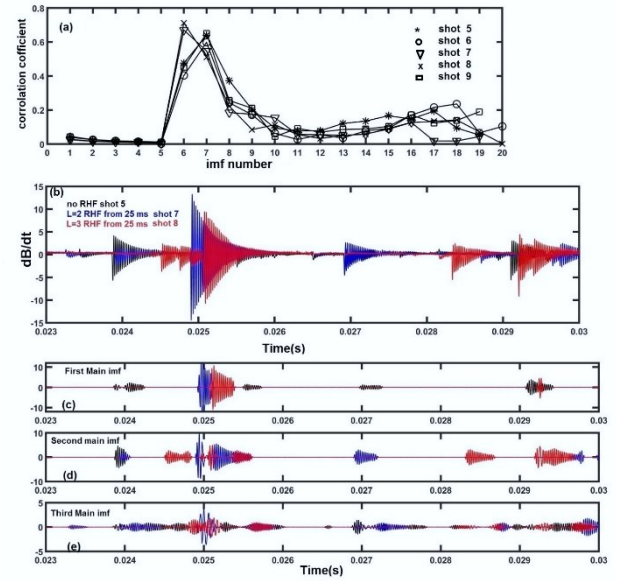


Figure7

In the resonance helical magnetic field application (RHF) imf6 is strongly correlated with correlation coefficient 0.67(shot7) and 0.71(shot8) for $l = 2/n = 1$ and $l = 3/n = 1$ RHF respectively. Figure 8a shows the time evolution of Mirnov signals in the ohmic discharge. The results show that the amplitude of the Mirnov signals is large and decays during the period from (24 to 25ms) and (29 to 30ms). The amplitude of these oscillations is low during (25-29ms) and it starts to decay in this period.

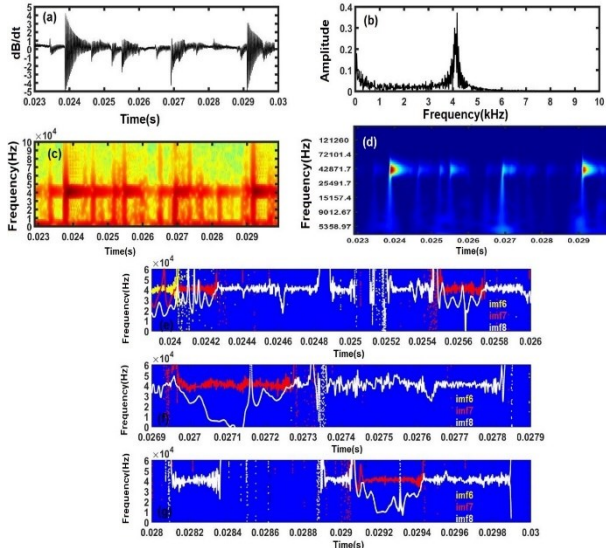


Figure 8

Calculation of correlation coefficients indicates that, in the ohmic discharge imf6, imf7 and imf8 are strongly correlated with the raw data. Instantaneous frequency of the imf6 indicates that, there is a very short time during the period from (23 to 24 ms) with frequency component at 40 kHz. The amplitude of the imf7 is lower than the imf6, and this mode oscillates with the same frequency. In addition, the oscillation period of imf7 is greater than imf6. This mode oscillates for example, during the period from (24 to 24.2 ms) and (25.4 to 25.8 ms). In addition, the MHD activity with the low amplitude can be seen at frequencies 10-30 kHz belong to the imf8 that oscillates for example, during the period from (23 to 24.2 ms) and (25.4 to 25.8 ms). The Short Time Fourier Transform (STFT) and Wavelet Transform (WT) methods show that the MHD activity has a broad range of frequencies below than 45 kHz. In these results, the frequencies are widely spread and the end effect is very prominent (see Fig 8c,8d). In the wavelet plot the low frequencies MHD activities are not clear and the appropriate scales should be chosen for analysis. As illustrated by FFT result there are some branches in frequency between 40-45 kHz in ohmic discharge. We can see that, there still exist the low frequencies less than 10 kHz in FFT result (see Fig 8b). The results presented above show that, the amplitude of the MHD oscillations change quickly in short period. This amplitude grows and drops rapidly and these burst oscillations repeat several times during the magnetic confinement of plasma. The large amplitude MHD activity led to a minor disruption and this high frequency oscillation then disappear. Figure 9a shows the oscillatory magnetic signals around the time 25ms after application of the $l = 2/n = 1$ resonant field. The amplitude of the MHD oscillations is amplified around the time 25 ms (Fig 7b shot7) and it is strongly suppressed during (26-27ms).

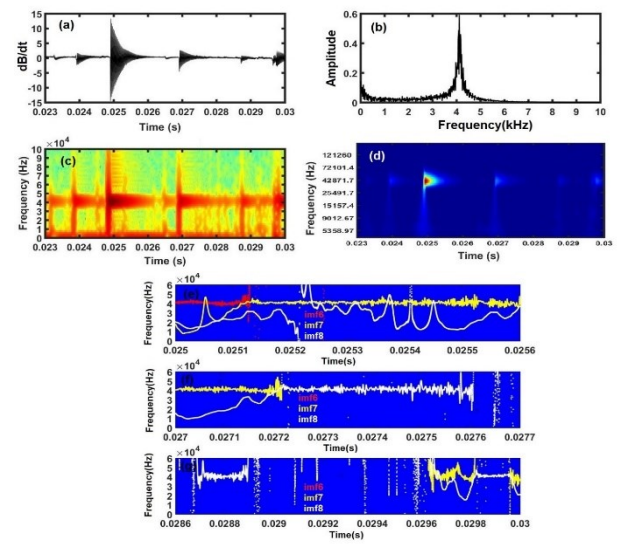


Figure 9

The HHT and WT results show that the amplitude of the MHD oscillation is completely damped and the oscillation frequency is dropped during the period from 26-27 ms after stopping the amplification. In the HHT spectrum results, the high amplitude MHD activity is represented with mode (imf6) that oscillates at 40 kHz frequency only during the period from 25 to 25.1ms (see Fig 7e). The second main imf (imf7) oscillates at frequencies between 10- 40 kHz in this period. On the other hand, we see that, imf7 oscillates at frequency 40 kHz with the low amplitude during the period from (25.1 to 25.6 ms), (27 to 27.2 ms) and (29.6 to 30 ms). In addition, the third main imf (imf8) oscillates at frequencies 20-30 kHz, for example during the period from 25 to 25.6 ms and 27 to 27.2 ms.

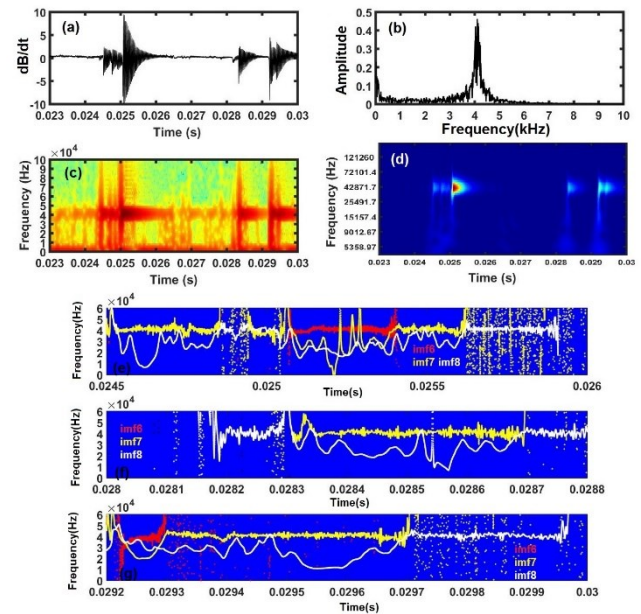


Figure 10

Figure 10a shows oscillatory Mirnov signals around the time 25ms after application of $l=3/n=1$ resonant field.

Figure 10e shows that, the first main imf (imf6) oscillates with high amplitude at 40 kHz frequency during the period from (25 to 25.5 ms) and (29.2 to 29.3 ms). The second main imf (imf7) oscillates for example during the period from (28.3 to 28.7 ms) and 29.3 to 29.7ms.

The third main imf (imf8), oscillates for example during the period from (25 to 25.5 ms) at frequencies between 20-30 kHz.

In the following, we study the effect of the resonance helical magnetic field effect on the spatial mode structures of MHD activity in the IR-T1 Tokamak plasma. In this experiment we used an array of Mirnov that consists of 12 discrete coils with a poloidal separation of 30° . As the sample rate of data acquisition is $0.5 \mu s$. In HHT method, one signal of that array was sufficient. In pervious section the signals were recorded with an Oscilloscope (four channels) with the sample rate 50 ns.

For analyzing RHF effect, Singular Value Decomposition (SVD), special Fourier series and HHT analysis were used.

We used shot (961011-7 for $l = 2/n = 1$ RHF) and shot (961011-8 for $l = 3/n = 1$). The resonance magnetic field was applied approximately at 25 ms for about 10 ms during the plasma current plateau. The plasma current was not completely flat, so very short time (24 -26 ms) was chosen for the analysis.

SVD can extract the spatial features of MHD modes in a form of eigenvectors called Principal axes [4].

PAs of the dominant poloidal MHD modes before application of $l = 2/n = 1$ RHF during the period from (24-25 ms), and after application of it, during the period from (25-25.2ms), (25.2-26ms) are respectively shown in polar plots in Figures 11a ,11b and 11c. The middle plot corresponds to the dominant mode at the moment of applying the $l = 2/n = 1$ RHF. The spatial structure can be approximately identified as an $m = 2$ mode. The first and last mode can be identified as an $m = 4$ mode. The magnitudes of harmonics from $m = 1$ to $m = 4$ can be obtained using the spatial Fourier series. The spatial Fourier series decomposes the sine and cosine components of each mode from raw Mirnov signals [4].

Figure 11d shows the analysis results were performed on the time window (24-26 ms) by spatial Fourier series. The $m = 2$ mode has the highest magnitude among the other modes at the moment of applying the $l = 2/n = 1$ RHF. The $m = 1$ and $m = 4$ amplitudes dominant in the time interval before (24-25 ms) and after (25.2-26 ms) applying the $l = 2/n = 1$ RHF.

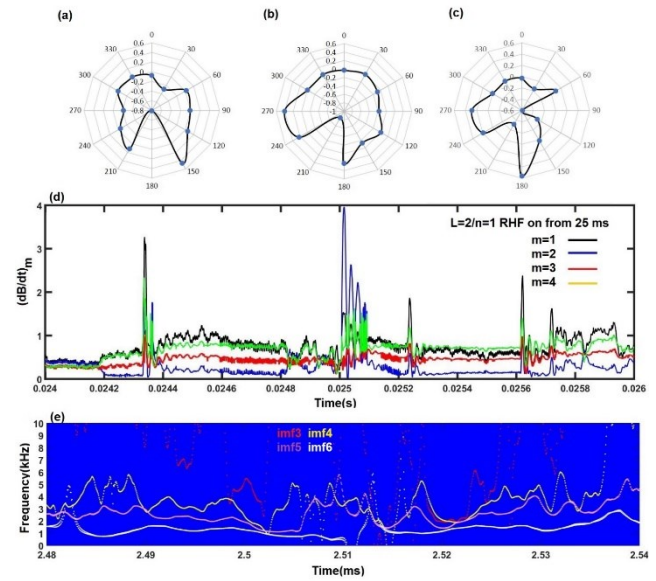


Figure11

Hilbert Transform (HT) of the third, fourth, fifth and sixth imfs in the time window (24-26 ms) has been shown in Figure 11e. We see dominant instantaneous frequencies for single Mirnov probe (210°) in this figure.

The results of HHT analysis show that, at the moment of applying the $l = 2/n = 1$ RHF, high frequency MHD mode at 40-50 kHz frequencies are amplified and then the frequency of these MHD mode decreased in a very short time.

We continued this analysis to determine the spatial mode structures of MHD activity after application of $l = 3/n = 1$ RHF. PAs of the dominant poloidal MHD modes before application of $l = 3/n = 1$ RHF during the period from (24-25 ms), and after application of it, during the period from (25-25.2 ms), (25.2-26 ms) are respectively shown in polar plots in Figures 12a ,12b and 12c. The middle plot corresponds to the dominant mode on the time during (25-25.2 ms) after application of the $l = 3/n = 1$ RHF.

The spatial structure is identified as an $m=3$ mode and the first and last mode can be identified as an $m = 4$ mode. Figure 12d shows the analysis results were performed on the time window (24-26 ms) by spatial Fourier series. The $m = 3$ mode has the highest magnitude among the other modes on the time during (25 – 25.2ms) after application of the $l = 3/n = 1$ RHF. The $m = 1$ and $m = 4$ amplitudes dominant in the time interval before (24 – 25 ms) and after (25.2 – 26 ms) applying the $l = 3/n = 1$ RHF.

The results of HHT analysis show that, at the moment of applying $l = 3/n = 1$ RHF, the dominant frequencies are amplified in the range 40-50 kHz (Fig12e).

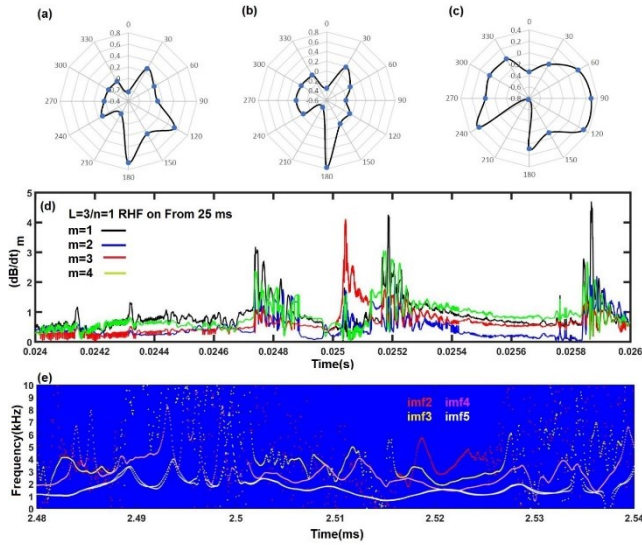


Figure12

The other low frequencies modes can be seen in the range 20-30 kHz in this figure.

CONCLUSION

The effect of a resonant helical magnetic field (RHF) on IR-T1 tokamak plasma confinement is studied using Hilbert-Huang transform (HHT) analysis. The results show that, in the ohmic and RHF discharges the main MHD mode belong to the magnetic island, that oscillate around 40 kHz frequency. In the MHD activity analysis the lower frequencies can be seen in the range of 10-30 kHz. We see that, amplitude and frequency spectrum of the coupling MHD modes separated by the HHT analysis and the MHD oscillations amplitude recognize in different periods. That means, HHT method can extract MHD activities with different amplitudes in the different times and then, the instantaneous frequencies (IFs) of these modes can be calculated by Hilbert Transform (HT). For example, the $m = 4$ poloidal MHD mode is the dominant MHD activity in IR-T1 tokamak plasma on

the time during (24-26 ms) that oscillates around 40 kHz frequency. On the time during (24-26 ms), the poloidal modes $m = 2$ and $m = 3$ is amplified with the same Frequency after application of $l = 2/n = 1$ and $l = 3/n = 1$ RHF respectively. As a comparison of WT and HHT analysis the Hilbert spectrum has much better frequency definition.

Amplitude modulation of Mirnov oscillations in IR-T1 tokamak generate intra-wave frequency modulation and in the Hilbert spectrum analysis, this effect is small compared to the STFT and WT spectrums. Moreover, the time evolution of Mirnov signal indicates that, the amplitude of MHD activity changes in short period. This amplitude grows and drops rapidly and this burst oscillation repeat several times during the discharge. Each burst constituting a minor disruption which is accompanied by decrease in plasma current amplitude. The resonance magnetic field was applied for about 10 – 15 ms during the plasma current plateau. Since the plasma current was not completely flat, so it is very difficult to study the RHF effect in many time intervals. For this reason, a very short time before (24 – 25 ms) and after (25 – 26 ms) applying RHF was chosen for the analysis. The main effect of RHF application on the IR-T1 Tokamak during a low-q ohmic discharge ($q(a) < 5$) is a few milliseconds suppression in MHD activity after amplification of it. In the application of RHF the $m = 2$ MHD mode amplifies at 40 kHz frequency after application of $l = 2/n = 1$ resonant field. The suppression of Mirnov oscillations does not occur immediately when the RHF applied.

In this case we can see that, $m = 2$ MHD mode are suppressed for a few milliseconds after amplification. On the other hand, after application of $l = 3/n = 1$ resonant field the amplitude of $m = 3$ MHD activity are amplified more than other MHD modes at 40 kHz frequency. The $m = 3$ MHD mode are strongly suppressed for a few milliseconds after amplification similar to the $m = 2$ mode.

REFERENCES

- [1] T. Hender *et al.*, "Effect of resonant magnetic perturbations on COMPASS-C tokamak discharges," vol. 32, no. 12, p. 2091, 1992.
- [2] D. Roberts, J. De Villiers, J. Fletcher, J. O'Mahony, and A. J. N. f. Joel, "Major disruptions of low aspect ratio tokamak plasmas caused by thermal instability," vol. 26, no. 6, p. 785, 1986.
- [3] J. Adam *et al.*, "Plasma physics and controlled nuclear fusion research," in *Proc. 5th Int. Conf.(Tokyo, 1974)*, 1975, vol. 1, p. 65.
- [4] S. Elgriw, D. Liu, T. Asai, A. Hirose, and C. J. N. F. Xiao, "Control of magnetic islands in the STOR-M tokamak using resonant helical fields," vol. 51, no. 11, p. 113008, 2011.
- [5] D. Roberts, D. Sherwell, J. Fletcher, G. Nothnagel, and J. J. N. f. De Villiers, "Major disruptions induced by helical coils on the Tokoloshe tokamak," vol. 31, no. 2, p. 319, 1991.
- [6] P. Savrukhn, E. Lyadina, D. Martynov, D. Kislov, and V. J. N. f. Poznyak, "Coupling of internal $m = 1$ and $m = 2$ modes at density limit

- disruptions in the T-10 tokamak," vol. 34, no. 3, p. 317, 1994.
- [7] B. Waddell, B. Carreras, H. Hicks, J. Holmes, and D. J. P. R. L. Lee, "Mechanism for major disruptions in tokamaks," vol. 41, no. 20, p. 1386, 1978.
- [8] Q. Hu *et al.*, "Effect of externally applied resonant magnetic perturbations on resistive tearing modes," vol. 52, no. 8, p. 083011, 2012.
- [9] M. Nave and J. J. N. F. Wesson, "Mode locking in tokamaks," vol. 30, no. 12, p. 2575, 1990.
- [10] J. Wesson and D. J. Campbell, *Tokamaks*. Oxford university press, 2011.
- [11] W. Jin *et al.*, "Dependence of plasma responses to an externally applied perturbation field on MHD oscillation frequency on the J-TEXT tokamak," vol. 55, no. 3, p. 035010, 2013.
- [12] D. J. J. o. t. I. o. Gabor, "Electrical Engineers-Part III: Radio and Communication Engineering," vol. 93, no. 429, p. 39, 1946.
- [13] I. Daubechies, *Ten lectures on wavelets*. SIAM, 1992.
- [14] N. E. Huang *et al.*, "The empirical mode decomposition and the Hilbert spectrum for nonlinear and non-stationary time series analysis," vol. 454, no. 1971, pp. 903-995, 1998.
- [15] J. Terradas, R. Oliver, and J. J. T. A. J. Ballester, "Application of statistical techniques to the analysis of solar coronal oscillations," vol. 614, no. 1, p. 435, 2004.
- [16] J. Kurzyna *et al.*, "Spectral analysis of Hall-effect thruster plasma oscillations based on the empirical mode decomposition," vol. 12, no. 12, p. 123506, 2005.
- [17] A. Kakurin and I. J. P. p. r. Orlovsky, "Empirical mode decomposition method for investigating the structure of large-scale MHD instabilities in a tokamak," vol. 30, no. 5, pp. 370-375, 2004.
- [18] A. Kakurin and I. J. P. p. r. Orlovsky, "Hilbert-Huang transform in MHD plasma diagnostics," vol. 31, no. 12, pp. 1054-1063, 2005.
- [19] R. Jha, D. Raju, and A. J. P. o. p. Sen, "Analysis of tokamak data using a novel Hilbert transform based technique," vol. 13, no. 8, p. 082507, 2006.
- [20] R. Coelho, D. Alves, and C. J. R. o. s. i. Silva, "Magnetohydrodynamic and turbulence activity analysis in the ISTTOK tokamak using empirical mode decomposition," vol. 77, no. 10, p. 10F512, 2006.
- [21] Y. Liu, Y. Tan, H. Xie, W. Wang, and Z. J. R. o. S. I. Gao, "Time-frequency analysis of non-stationary fusion plasma signals using an improved Hilbert-Huang transform," vol. 85, no. 7, p. 073502, 2014.
- [22] A. Storelli *et al.*, "Comprehensive comparisons of geodesic acoustic mode characteristics and dynamics between Tore Supra experiments and gyrokinetic simulations," vol. 22, no. 6, p. 062508, 2015.
- [23] G. Huang, Y. Su, A. Kareem, and H. J. J. o. E. M. Liao, "Time-frequency analysis of nonstationary process based on multivariate empirical mode decomposition," vol. 142, no. 1, p. 04015065, 2016.
- [24] M. Ghoranneviss, A. Hogabri, and S. J. N. f. Kuhn, "MHD activity at low q (a) in Iran Tokamak 1 (IR-T1)," vol. 43, no. 3, p. 210, 2003.
- [25] M. Lafouti, M. Ghoranneviss, S. Meshkani, and A. S. J. J. o. P. P. Elahi, "Low MHD activity using resonant helical field and limiter biasing in IR-T1 tokamak," vol. 79, no. 5, pp. 765-770, 2013.